Available online at www.sciencedirect.com
SCIENCE DIRECT®
Thermochimica Acta 421 (2004) 19–24
thermochimica acta
www.elsevier.com/locate/tca

Biomimetic complexes: thermal stability, kinetic study and decomposition mechanism of Co(II)-, Ni(II)- and Cu(II)-4(5)-hydroxymethyl-5(4)-methylimidazole complexes

S. Materazzi [a,*], S. Aquili [a], S. De Angelis Curtis [a], S. Vecchio [b], K. Kurdziel [c], F. Sagone [a]

[a] *Department of Chemistry, University of Rome,"La Sapienza" p.le A.Moro, 5-00185 Rome, Italy*
[b] *Department of Chemical Engineering (I.C.M.M.P.M.), University of Rome, "La Sapienza" Via del Castro Laurenziano, 7-00161 Rome, Italy*
[c] *Institute of Chemistry, Swietokrzyska Academy, Checinska, 5-25-020 Kielce, Poland*

Received 3 November 2003; received in revised form 20 February 2004; accepted 28 February 2004
Available online 8 May 2004

Abstract

A thermoanalytical study of 4(5)-hydroxymethyl-5(4)-methylimidazole complexes with divalent cobalt, nickel and copper, with a general formula $ML_4(NO_3)_2$ is reported: the thermal stability and the decomposition steps were determined by thermogravimetry (TG) and derivative thermogravimetry (DTG). The released products, due to the thermal decomposition, were analyzed by on-line coupling a FT-IR spectrometer to the thermobalance; the so obtained evolved gas analysis (EGA) allowed to prove the proposed decomposition steps. The decomposition kinetics was examined by using the Flynn–Wall–Ozawa and Kissinger methods. From the former method the *E* dependencies were presented and connected with the corresponding steps mass loss; from the latter method the activation energies and the pre-exponential factor were computed.

Keywords: Coordination compounds; Imidazole derivatives; Hydroxymethyl-methylimidazole; TGA; Coupled TG–FT-IR; EGA; Transition metal ions complexes; Decomposition kinetics

1. Introduction

The bidentate nature of the imidazole ligands with the hydroxymethyl substituent, in which, apart from the pyridynic nitrogen atom, the oxygen atom of the $–CH_2OH$ group is another electron donor, explains the high stability of transition metal ion complexes with this molecules [1–3]. The hydroxymethyl substituent is also known to form more stable complexes than the corresponding alkyl substituents [4–6].

In two recent articles [7,8], the synthesis, the crystal structure and the spectroscopic properties of 4(5)-hydroxymethyl-5(4)-methylimidazole complexes with divalent cobalt, nickel and copper, with a general formula $ML_4(NO_3)_2$, has been reported.

To complete the characterization of these biomimetic compounds, a thermoanalytical study was performed and the results are here reported: the thermal stability and the decomposition steps were determined by thermogravimetry (TG) and derivative thermogravimetry (DTG). The released products, due to the thermal decomposition, were analyzed by on-line coupling a FT-IR spectrometer to the thermobalance; the so obtained evolved gas analysis (EGA) allowed to prove the proposed decomposition steps.

Flynn–Wall–Ozawa (FWO) [9,10] and Kissinger [11,12] kinetic methods were used in the present work to evaluate the activation energy. From the FWO method the *E* dependencies were reported and connected with the corresponding mass loss step, while from the Kissinger method the activation energies and the pre-exponential factor were considered.

2. Experimental

2.1. Syntheses of the complexes

All the complexes of general formula $ML_4(NO_3)_2$ (where M = Co(II), Ni(II) or Cu(II)) were synthesized by following the same procedure reported in the literature [7,8].

* Corresponding author. Tel.: +39-06-499-13616; fax: +39-06-445-3953.
E-mail address: stefano.materazzi@uniromal.it (S. Materazzi).

0040-6031/$ – see front matter © 2004 Elsevier B.V. All rights reserved.
doi:10.1016/j.tca.2004.02.020

The hydrochloride 5-hydroxymethyl-4-methylimidazole (Aldrich, Europe) was alkalized with a $KHCO_3$ solution. The free imidazole base was extracted with 1-BuOH. To an aqueous solution of 8 mmol of the imidazole base, an aqueous solution containing 2 mmol of the particular metal nitrate was added.

The precipitated crystals resulted light-pink for the cobalt complex, dark-violet for the nickel complex and navy-blue for the copper complex.

X-ray spectroscopy confirmed the proposed structure of the precipitated complexes [7,8].

2.1.1. Elemental analysis

$CoL_4(NO_3)_2$: C 38.0% (30.04), H 5.2% (5.07), N 22.3% (22.19), O 25.3% (25.36); $NiL_4(NO_3)_2$: C 38.0% (30.04), H 5.1% (5.07), N 22.2% (22.19), O 25.4% (25.36); $CuL_4(NO_3)_2$: C 37.7% (37.76), H 5.0% (5.03), N 22.1% (22.03), O 25.2% (25.18).

2.2. Instrumental

The thermoanalytical curves were obtained using a Perkin-Elmer TGA7 thermobalance (range 20–1000 °C); the atmosphere was either pure nitrogen or air, at a flow rate of 100 ml min^{-1}; the heating rate was varied between 5 and 40 °C min^{-1}, with the best resolution achieved at a scanning rate of 10 °C min^{-1}.

To obtain the IR spectra of the gases evolved during the thermogravimetric analysis, the thermobalance was coupled with a Perkin-Elmer FT-IR spectrometer, model 1760X. The TGA7 was linked to the heated gas cell of the FT-IR instrument by means of a heated transfer line, the temperatures of the cell and of the transfer line being independently selected.

2.3. Kinetic methods of calculation

The non-isothermal kinetic analysis of the thermal decomposition stages was carried out using the data elaborated from the TG curves performed at different heating rates (from 2.5 to 20 °C min^{-1}).

The first proposed method [9,10] is based on the equation:

$$\ln \beta = -1.052\frac{E}{RT} - 5.311 + \ln\frac{AE}{R} - \ln\left[g(\alpha)\right] \quad (1)$$

where E is the activation energy, A the pre-exponential factor, R the gas constant, β the heating rate, α the degree of conversion, $g(\alpha) = \int_0^\alpha d\alpha/f(\alpha)$ the integral function of conversion and $f(\alpha)$ the differential function of conversion, which depends on the set of the considered kinetic models. For constant values of α the plot of $\ln \beta$ versus $1/T$ obtained at different heating rates should be a straight line whose slope enables the activation energy to be evaluated as a function of α.

The second method is based on the fact that the peak temperature is a function of the heating rate of the sample through the following (pseudo) first-order reaction

$$\ln\frac{\beta}{T_p^2} = -\frac{E}{RT_p} + \ln\frac{AR}{E} \quad (2)$$

where T_p is the peak temperature of the DTG curve and R the gas constant. This equation can be applied with a reasonable approximation even to an nth-order, regardless order. If the reaction proceeds under conditions where thermal equilibrium is always maintained, then a plot $\ln(\beta/T_p^2)$ versus $1/T_p$ gives a straight line with a slope equal to $-E/R$.

3. Results and discussion

Imidazole derivatives with two different substituents at positions 4 and 5 can exist in two tautomeric forms. The studied ligand occurs in the forms shown in Scheme 1 owing to anular tautomerism.

In the 4-hydroxymethyl-5-methylimidazole tautomer, the oxygen atom of the hydroxymethyl group adjacent to the nitrogen atom of the ring enables the formation of five-member chelating rings [7,8].

The complexes characterized in this work show a $ML_4(NO_3)_2$ general formula, with two monodentate molecules, co-ordinated through the 3-pyridynic nitrogen atom of the imidazole ring, while the remaining two molecules are bidentate ligands, the oxygen atom of the $-CH_2OH$ group being another electron donor that interacs with the metal ion.

Three main thermal decomposition steps are present in the TG profiles of the complexes (air flow), as shown in Fig. 1. The complexes are stable, with a TG plateau, up to 170 °C where the first releasing step occurs. It is followed by a second process in the temperature range 230–340 °C, with the final oxidation to give the metal oxide starting at 390 °C.

By referring to the structure, determined by X-ray spectroscopy [7,8], and by calculating the molecular weight corresponding to each releasing step, the decomposition mechanism shown in Scheme 2 can be proposed. In the first TG step, the release of the two non-coordinated $-CH_2OH$ groups can be calculated; the second process involves the loss of the four methyl groups and the breakdown of the coordination with the loss of the other two hydroxymethyl groups. The final decomposition to give the metal oxide is consequent to the loss of the complex coordination without

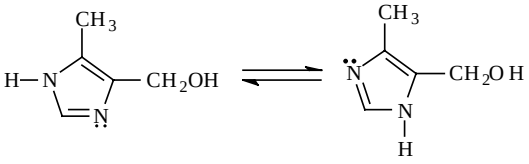

Scheme 1. Anular tautomerism of the 4(5)-hydroxymethyl-5(4)-methylmidazole molecule.

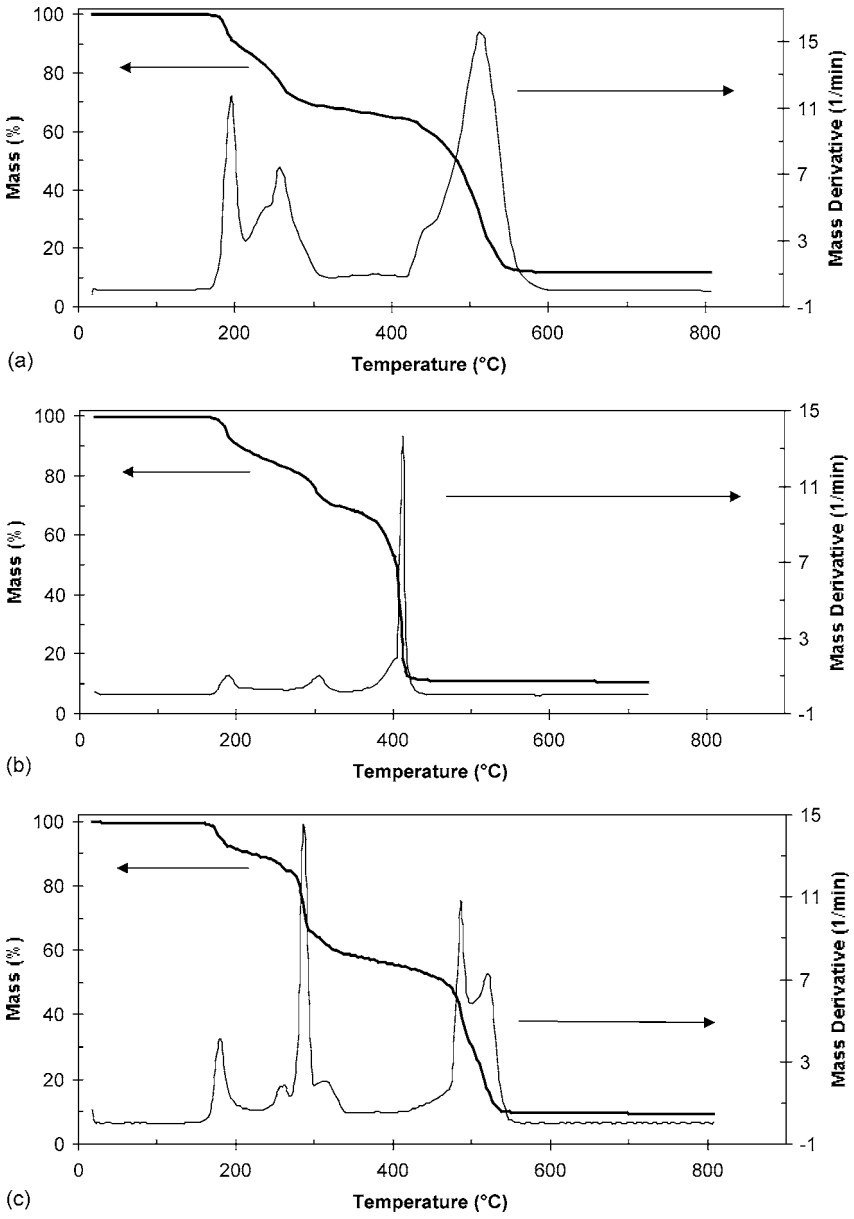

Fig. 1. TG (-) and DTG (—) curves of $CuL_4(NO_3)_2$ (a), $NiL_4(NO_3)_2$ (b) and $CoL_4(NO_3)_2$ (c) complexes. Heating rate: 10 °C min^{-1}; air flow at 100 ml min^{-1} rate.

a clear plateau usually found in other imidazole-derivative coordination compounds studied by our group [13–16].

The following equations are proposed:

$$M(C_5N_2H_8O)_4(NO_3)_2 \rightarrow M(C_5N_2H_8O)_2(C_4N_2H_4)_2(NO_3)_2$$

$$M(C_5N_2H_8O)_2(C_4N_2H_4)_2(NO_3)_2 \rightarrow M(C_3N_2H_4)_4(NO_3)_2$$

$$M(C_3N_2H_4)_4(NO_3)_2 \rightarrow \text{metal oxide}$$

When the purging flow is changed to inert gas (nitrogen or argon), only the final decomposition step is interested, with a shift of the decomposition temperature range to higher; no difference was shown in the temperature range 170–340 °C, so confirming two releasing steps instead of decompositions.

By the analysis of the evolved gases, performed by on-line coupling a FT-IR spectrometer to the thermobalance, the proposed decomposition steps can be confirmed.

As can be seen in the stacked plot of the spectra recorded in the temperature range 170–220 °C (Fig. 2), the IR bands are due to the release of the $-CH_2OH$ groups (not coordinated). In the temperature range 230–350 °C, corresponding to the second TG releasing process, the IR bands related to the loss of methyl groups appears in addition to the IR bands previous described.

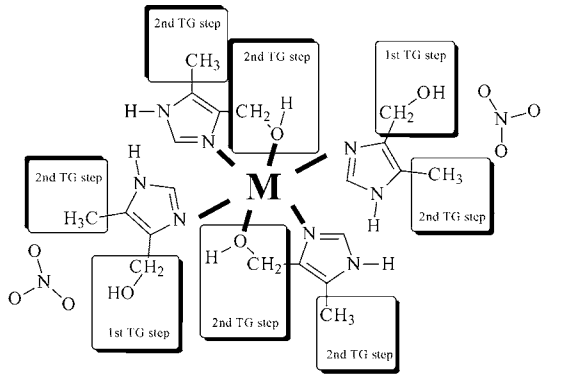

1st TG step ⟶ loss of two non-coordinated -CH_2OH

2nd TG step ⟶ loss of two coordinated -CH_2OH and of four -CH_3

3rd TG step ⟶ final decomposition to give the metal oxide

Scheme 2. The thermal decomposition mechanism for the $ML_4(NO_3)$ complexes.

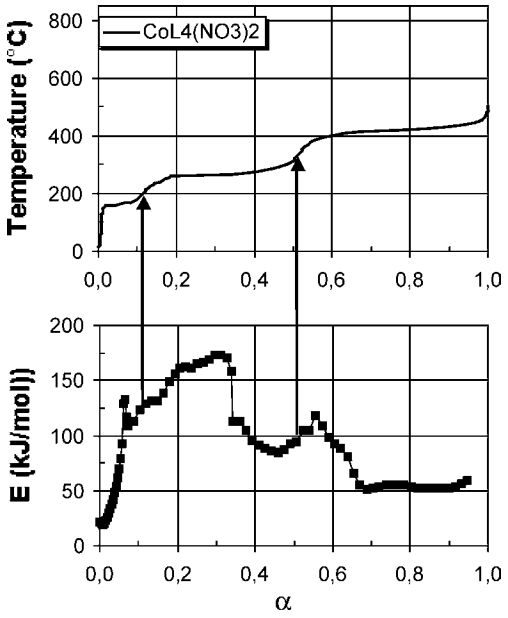

Fig. 3. TG curve for decomposition steps of $CoL_4(NO_3)_2$ at scanning rate of 10 °C min^{-1} (upper plot) compared to the dependence of the E values on α (lower plot).

The evolved gas analysis so confirms the proposed thermal decomposition pathway deduced by calculating the molecular weight loss from the TG traces.

By considering the final oxidation to give the metal oxides, Fig. 1 allows to propose a thermal stability scale, where $CuL_4(NO_3)_2 > CoL_4(NO_3)_2 > NiL_4(NO_3)_2$.

The thermal stability scale, as always for the coordination compounds, is exactly the opposite with respect to the stability scale for the complexes in solution reported by Kurdziel et al. [7,8]. However, in the first TG step an inversion is noted between the Co and the Ni complexes due to the different coordination sphere and the consequent different interactions of the oxygen of the non-coordinated –CH_2OH groups. Moreover, the Cu complex shows a lower stability for the second thermal release, the Ni complex being the last one to lose the hydroxymethyl and the methyl groups.

Figs. 3–5 compare the dependence of E on α against the experimentally obtained mass loss curve for all the examined complexes. The evaluated E-dependencies sometimes show drastic drops in the E values usually due to a computational artefact [17]. In fact, they occur at the point of transition from one mass loss step to another one, when the reaction rate shows a marked decrease.

The first decomposition step ($\alpha < 0.1$) shows an increase of the activation energy for the Cu and Co complexes (from

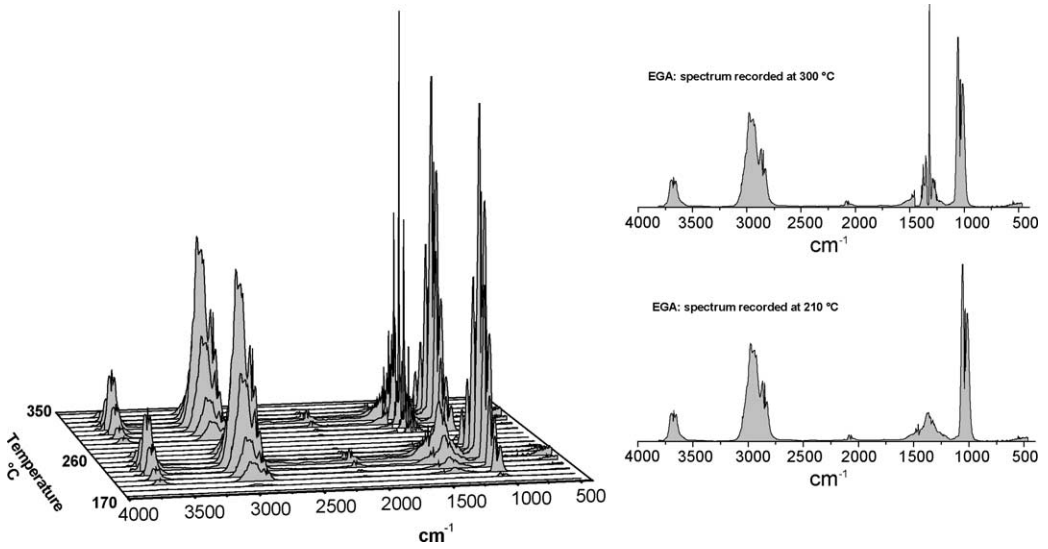

Fig. 2. Infrared spectra of the TG evolved gases for the decomposition of $ML_4(NO_3)_2$ complexes in the temperature range 300–400 °C. Resolution: 8 cm^{-1}–10 scans per spectrum.

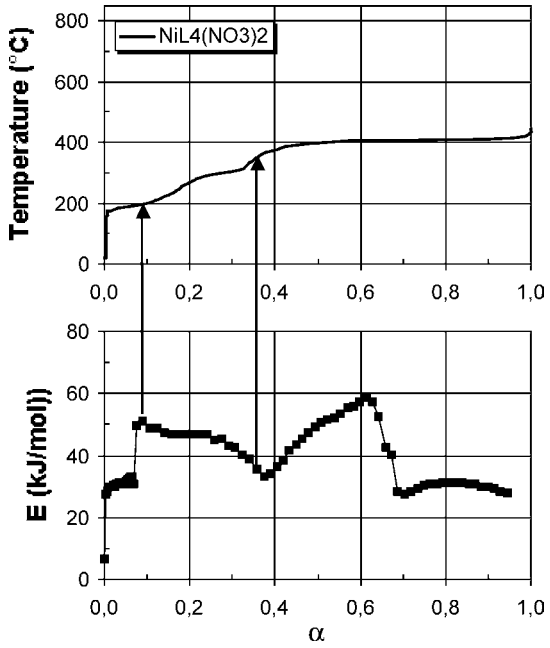

Fig. 4. TG curve for decomposition steps of $NiL_4(NO_3)_2$ at scanning rate of 10 °C min^{-1} (upper plot) compared to the dependence of the E values on α (lower plot).

48 to 142 kJ mol^{-1} and from 23 to 132 kJ mol^{-1}, respectively) while for the $NiL_4(NO_3)_2$ E is practically constant (31 ± 1 kJ mol^{-1}).

The activation energy increase at the beginning of the second step for Cu and Co complexes ($0.10 < \alpha < 0.45$) from

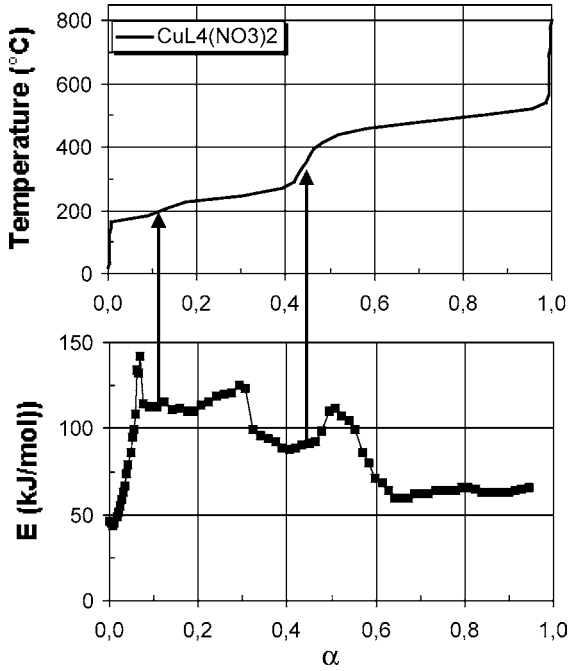

Fig. 5. TG curve for decomposition steps of $CuL_4(NO_3)_2$ at scanning rate of 10 °C min^{-1} (upper plot) compared to the dependence of the E values on α (lower plot).

Table 1
Activation energies obtained from Kissinger method (Eq. (2)) for all the studied complexes

Complex	Stages	E (kJ mol^{-1})	ln A (min^{-1})	r^2
$CoL_4(NO_3)_2$	I	93.1 ± 2.8	16.2 ± 0.5	0.9939
	II	148.5 ± 3.5	26.2 ± 0.7	0.9955
	III	54.9 ± 2.1	9.6 ± 0.5	0.9915
$NiL_4(NO_3)_2$	I	33.7 ± 1.6	5.9 ± 0.3	0.9889
	II	47.2 ± 1.5	8.3 ± 0.4	0.9975
	III	38.5 ± 1.8	6.6 ± 0.3	0.9925
$CuL_4(NO_3)_2$	I	94.8 ± 2.8	16.7 ± 0.6	0.9905
	II	111.9 ± 3.6	19.5 ± 0.8	0.9977
	III	69.7 ± 1.7	12.2 ± 0.6	0.9913

The associated uncertainties were also given as standard deviations.

113 to 125 kJ mol^{-1} and from 129 to 170 kJ mol^{-1}, respectively. For $NiL_4(NO_3)_2$ E decreases from 51 to 34 kJ mol^{-1} in the range $0.10 < \alpha < 0.39$.

At the end of the third decomposition step the process evidently accelerates and all the complexes lose more than 50% of mass in the temperature range ~370–600 °C. For all the studied complexes, the highest decomposition rates were reached at the end of the third step ($E < 70$ kJ mol^{-1}, $\alpha > 0.70$), with only a slight change in the activation energy.

On the basis of these results, the proposed stability scale is confirmed.

The activation energies obtained from Eq. (2) are listed in Table 1. These values are in good agreement with the middle calculated ones, reported in Figs. 3–5 for all decomposition steps.

The final conclusion is that the second step shows higher E values with both methods and represents the rate-determining step.

References

[1] T.J. Lane, C.S.C. Quinlan, K.P. Quinlan, J. Am. Chem. Soc. 82 (1960) 2994.
[2] K.S. Patel, I.M. Bhatt, D.P. Dani, Indian Chem. Soc. LIV (1977) 1007.
[3] M. Rzepka, W. Surga, Pol. J. Chem. 67 (1993) 2121.
[4] J. Kulig, K. Kurdziel, B. Barszcz, B. Lenarcik, Pol. J. Chem. 65 (1991) 2159.
[5] J. Kulig, B. Barszcz, B. Lenarcik, Pol. J. Chem. 66 (1992) 79.
[6] B. Barszcz, J. Kulig, J. Chem. Soc., Dalton Trans. (1993) 1559.
[7] K. Kurdziel, T. Glowiak, J. Jezierska, Polyhedron 21 (2002) 1857.
[8] K. Kurdziel, T. Glowiak, J. Jezierska, Inorg. Chem. Commun. 6 (2003) 459.
[9] T. Ozawa, Bull. Chem. Soc. Jpn. 38 (1965) 1881.
[10] J.H. Flynn, L.A. Wall, Polym. Lett. 4 (1969) 323.
[11] H.E. Kissinger, Anal. Chem. 29 (1957) 1702.
[12] H.E. Kissinger, J. Res. Natl. Bur. Standard A: Phys. Chem. 57 (1956) 217.
[13] S. Materazzi, E. Vasca, Thermochim. Acta 373 (2001) 7.

[14] S. Materazzi, K. Kurdziel, U. Tentolini, A. Bacaloni, S. Aquili, Thermochim. Acta 395 (2003) 137.
[15] S. Materazzi, G. D'Ascenzo, S. Aquili, K.M. Kadish, J.L. Bear, Thermochim. Acta 397 (2003) 129.
[16] S. Materazzi, S. Aquili, C. Bianchetti, G. D'Ascenzo, K.M. Kadish, J.L. Bear, Thermochim. Acta. 409 (2004) 145.
[17] T. Sell, S. Vyazovkin, C. Wight, Combust. Flame 119 (1999) 174.